EXCESSIVE YAW BEHAVIOUR OF COMMERCIAL VEHICLES, A FUNDAMENTAL APPROACH.

Joop P. Pauwelussen
TNO-Automotive & Technical University Delft
E-mail : pauwelussen@wt.tno.nl
The Netherlands
ID#: 414

1. ABSTRACT

Rollover of trucks is a major problem. In The Netherlands, it occurs about twice a week, and the number is increasing. A factor contributing to this might be the maximised speed of commercial vehicles, not stimulating the driver to reduce this speed in potentially critically conditions.
Several causes can be identified, one of them is excessive yaw behaviour of truck or trailer posing major difficulties for the driver, and likely to occur at lateral accelerations far below the static tilting boundary.

This paper first treats yaw-stability for a single heavy vehicle in a fundamental way. The analysis will be based on the full non-linear vehicle behaviour where critical (stationary) points are discussed within a phase plane representation. Local behaviour of trajectories around these points will be analysed yielding the type of (in-)stability, for all possible combinations of effective tyre behaviour (incorporating suspension characteristics).
These effects will also be presented in terms of the handling-diagram representation, showing the lateral acceleration under stationary conditions in terms of steering angle and road curvature. The shape of this diagram can be interpreted in terms of steering sensitivity of the vehicle.
The results will be extended to tractor-trailer combinations, where the previous results applied to each of the articulations together lead to an understanding of stability of the full vehicle combination.
The different types of excessive yaw modes (jack-knifing, trailer swing) of the combination will be discussed as related to the steering characteristics of the separate parts, and with reference to various vehicle parameters.

2. YAW STABILITY OF A SINGLE VEHICLE.

We start with a discussion of the yaw stability of a single vehicle. Clearly, this item is thoroughly discussed in many textbooks, however in most cases based on linear tyre-characteristics. In this paper, focus will be on non-linear tyre characteristics, and the appropriate analysis approaches will be reviewed first. In the next section, these approaches will be extended to articulated vehicles.

We start with the well-known single-track bicycle model for plane behaviour of a single vehicle in terms of lateral velocity v and yaw-rate r:

$$\begin{aligned} m(\dot{v} + u.r) &= F_{y1} + F_{y2} \\ J_z.\dot{r} &= a.F_{y1} - b.F_{y2} \end{aligned} \qquad (1)$$

with vehicle forward velocity u, vehicle mass m, and J_z the polar moment of inertia (yaw moment of inertia). Effective axle lateral forces are denoted as F_{yi} for i=1,2 for front and rear axle, respectively. The parameters a and b are the distances between the vehicle cog and the front and rear axle, respectively. The effective lateral axle forces include the combined performance of tyre characteristics as well as suspension characteristics (such as for special axle configurations), where suspension compliances, lateral load transfer etc. may be accounted for.
Special axle configurations such as with dual tyres or including two- or three axle combinations may also be accounted for by this model, as observed by Winkler [6]. More specific, the axle configurations as mentioned effect the steering axle on top of the influence of the lateral acceleration. In other words, the necessary steering angle to negotiate a curve is not only depending on the lateral acceleration a_y but also on the radius of curvature, independent of a_y.
Both in the linear case (linear tyres) as in the case of nonlinear load dependency of the tyre lateral characteristics, this can be accounting for (exact for linear tyres, a good approximation for the nonlinear

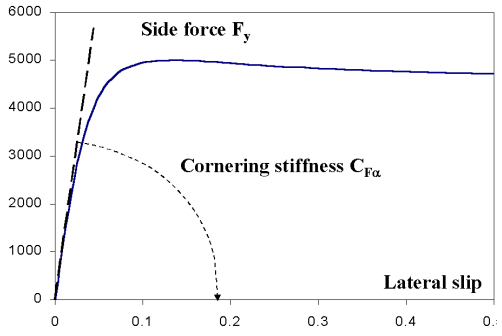

Figure 1.: Nonlinear axle characteristics

load dependency) by shifting the front axle more to the front, and the rear axle-configuration slightly further to the rear.
The set of equations (1) is formulated in terms of two dependent variables, v and r. The lateral axle forces F_{y1} and F_{y2} depend on the slip angles α_1 and α_2:

$$F_{y1} = F_{y1}(\alpha_1)\,;\; F_{y2} = F_{y2}(\alpha_2) \qquad (2)$$

where we recall that these functions are highly non-linear, see figure 1, with the slip-angles given by

$$\alpha_1 = \delta - \frac{v + ar}{u}\;;\; \alpha_2 = -\frac{v - br}{u} \qquad (3)$$

with steering angle δ. That means that the state variables v and r can be replaced by the slip angles α_1 and α_2, resulting in:

$$\begin{pmatrix}\dot{\alpha}_1\\ \dot{\alpha}_2\end{pmatrix} = \frac{u}{l}.(\alpha_2 - \alpha_1 + \delta)\begin{pmatrix}1\\1\end{pmatrix} - \frac{g}{u}.\begin{pmatrix}f_{y1}\\ f_{y2}\end{pmatrix} + \begin{pmatrix}\dot{\delta}\\ 0\end{pmatrix} \qquad (4)$$

for normalised axle characteristics

$$f_{y1}(\alpha_1) = \frac{F_{y1}(\alpha_1)}{F_{z1}}\;;\; f_{y2}(\alpha_1) = \frac{F_{y2}(\alpha_2)}{F_{z2}} \qquad (5)$$

with axle loads F_{zi}, front and rear (i=1, 2). The dynamic behaviour of solutions of (5) may be studied in the phase plane, with state vector (α_1, α_2). Clearly, solution lines (trajectories) will either move to the singular points corresponding to steady state solutions of (4) or vanish to infinity. Some examples are shown in figures 2 – 4 below, corresponding to the following cases:

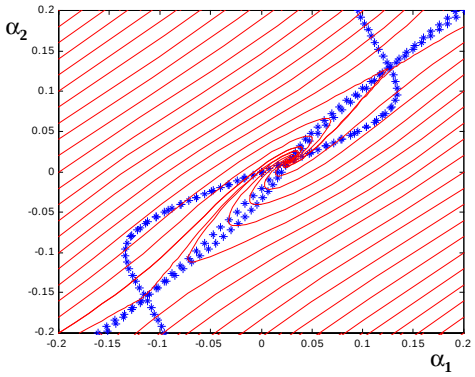

Figure 2.: Phase plane representation understeered vehicle.

- understeered vehicle
- stable oversteered vehicle (below critical speed)
- unstable oversteered vehicle (beyond critical speed: $v < v_{crit}$)

Axle characteristics have been chosen such that three steady state solutions may exist. The same figures also show (in blue) the isoclines corresponding to a fixed slope of the solution curves (horizontal, vertical, under 45°). Intersections of these isoclines coincide with the singular points.

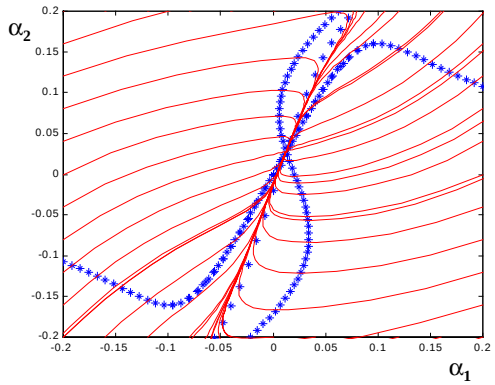

Figure 3.: Phase plane representation Oversteered vehicle, $v < v_{crit}$

In case of an understeered vehicle, a stable focus arises in the middle with two unstable saddle points

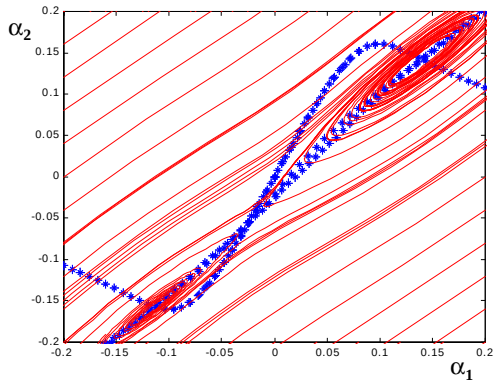

Figure 4.: Phase plane representation Oversteered vehicle, $v > v_{crit}$

for the other two steady state conditions. This means that initial conditions should not be too far off from this stable point in order to guarantee the solution to approach this point as $t \to \infty$. In other words, the attraction area of this point is bounded with boundary built up from the manifolds of both saddle points. Consequently, the non-stable singular points

determine the attraction area of the stable steady state solution.

In case of an oversteered vehicle for sufficiently large speed, the intermediate steady state solution has turned into an unstable point (as expected) being a saddle point in between two stable focus points. This unstable point is known to turn into a stable one with decreasing vehicle speed, as observed in figure 3. This time, a stable two-tangent node is obtained as singular point.

Sofar, we have discussed singular (steady state) points and the type of stability with distinction in divergent instability (saddle points), oscillatory (in-) stability (focus point), convergent stability (two-tangent node), etc.

We shall treat both aspects more in detail. For further interpretation of stability and the occurrence of several steady state solutions in terms of forward speed u and steering angle δ, the so-called **handling diagram** offers many advantages.

From the equations (1) under steady state conditions, one easily finds:

$$f_{y1}(\alpha_1) = f_{y2}(\alpha_2) = \frac{u^2}{gR} = \frac{K}{mg} \text{ (in } a_y) \qquad (6)$$

for pathradius R and acceleration of gravity g. Inverting (6) with:

$$g_i(a_y) = inv[f_{yi}(\alpha_i)](a_y) \quad ; \text{i=1,2} \qquad (7)$$

being now multivalued functions in the lateral acceleration a_y (in g's, i.e. K/(mg)), i.e. where both single-valued branches may be treated separately.

It follows using (3) that

$$\alpha_1 - \alpha_2 = \delta - \frac{l}{R} = g_1(a_y) - g_2(a_y) \equiv h(a_y) \qquad (8)$$

with l = a + b. Considering this relationship as a_y versus steering angle δ, one recognises the handling characteristic expressing the change of steering angle in lateral acceleration. A positive slope of δ versus a_y is usually related to understeer behaviour whereas a negative slope indicates understeer behaviour. The result of this exercise is shown in figure 5 for a certain combination of axle characteristics, indicating clearly the strong impact of axle (i.e. tyre) characteristics on vehicle steering performance. This result (handling curve) will be merged with another diagram having the ordinate K/(mg) yielding the so-called handling diagram. From (6), one observes that the side force K depends linearly on the path curvature (a+b)/R ≡ l/R, i.e. corresponding to a family of straight lines with slope proportionally to the square of the vehicle speed. According to (8), these curves and the diagram in figure 5 combine to produce the steer angle as the horizontal distance between the handling curve (figure 5) and these straight lines, see figure 6.

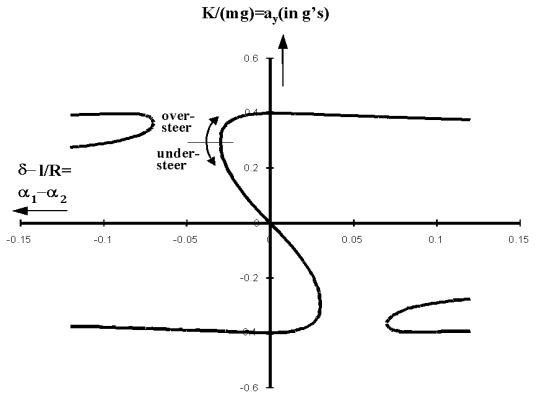

Figure 5.: Handling diagram, first step

For a better understanding, the application of the handling diagram as depicted in figure 6, is discussed step by step. Assume a path-radius R_1 (i.e. path

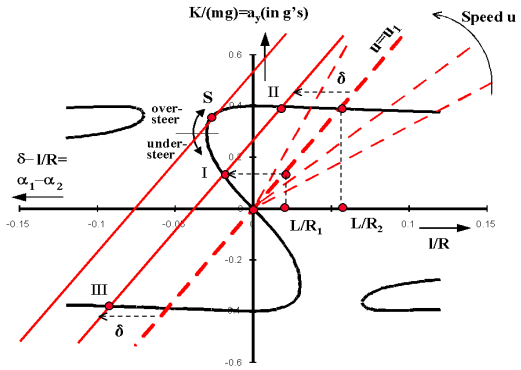

Figure 6.: Handling diagram

curvature l/R_1) and a vehicle forward speed u_1. That means that the point (l/R, K/(mg)) is lying on the straight line with slope $(u_1^2/(g.l))$. Because of (8), applying a steering angle δ means that this line is shifted to the left over a horizontal distance δ.

As a result, steady state solution I is found, lying in the understeer region. For very small speed u, the corresponding straight line is almost coinciding with the horizontal axis, and consequently, the necessary steering angle to reach the origin equals l/R, the Ackermann angle. For speed u_1 and steering angle δ, three steady state solutions arise, denoted as I, II and III as long as δ is not too large. For a certain value of δ, $\delta = \delta_S$ the point S is reached (see figure 6) and beyond this value, the number of three steady state solutions drops down to 1 (which must be unstable).

Now assume the steering angle δ to be chosen below δ_S but close to it, and consider the resulting steady state solution I. Slightly increasing the lateral acceleration a_y implies increase of the steering angle in order to reach a new steady state solution. That means that I is stable as long as it is situated below S. In the same way one may conclude that, for the steady state solution II lying above S, increase of a_y would involve reduction of steering angle δ yielding a self-reinforcing affect (further increase of a_y), leading to yaw-instability.
This kind of instability can only occur if the vehicle behaves oversteered, i.e. when the slope of the handling curve is positive. Decreasing of the speed u leads to increase of the lateral acceleration where the steering angle is maximal. This maximum steering angle increases as well with decreasing u. Consequently, stability is improved.

Instability occurs in points II and III where the slopes are negative but where one of the axle characteristics (rear axle) shows a downward slope at the α concerned.
Analysis of the coefficients of the characteristic equation for the disturbed motion around an equilibrium point reveals the question of stability. Also, the nature of stability (monotonous, oscillatory) follows from these coefficients. This is reflected in the type of singular points (node, saddle, focus) as discussed earlier. This analysis has been carried out yielding the diagram in figure 7.

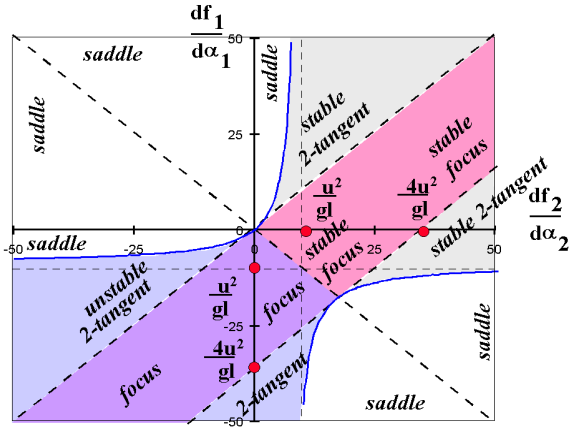

Figure 7.: Stability areas and types of singular points

This diagram shows areas with similar type of singular points, depending on the value of cornering stiffness for the normalised axle characteristics. The boundaries of these areas depend on vehicle velocity u. Clearly, the part of the diagram for large negative values of these normalised cornering stiffnesses are only relevant for theoretical reasons, i.e. to illustrate the typical pattern of these areas. However, observe that the cases in the lower half of the diagram may occur for excessive vehicle behaviour for small u.
The stable and unstable regions excluding the saddle points are distinguished by a slightly lighter colour for the stable regions. Figure 7 reveals that stable steady state solutions are either two-tangent nodes or a stable focus.
A stable oversteered vehicle with positive axle cornering stiffnesses will correspond to a two-tangent node, i.e. with disturbances (such as in case of a J-turn) approaching it in a monotonous way without oscillations. As long as u^2 is bounded by $g.l.[f_{y2,\alpha}(\alpha_2) - f_{y1,\alpha}(\alpha_1)]$ in the understeer region, the steady state solution corresponds to a stable focus. Beyond this speed, this focus turns into a stable two-tangent node. In the situation of excessive understeer ($f_{y1,\alpha}(\alpha_1) < 0$), a same distinction can be made.
These regions are more or less flipped to the unstable area leading to unstable two-tangent nodes and unstable focus. In all the other cases, the singular point is a saddle point.

3. YAW STABILITY OF ARTICULATED VEHICLES.

Now let us discuss an articulated vehicle, as schematically shown in figure 8, below.
Roll-motion will be neglected, steer and slip angles will be assumed small, driving forces and braking forces are small compared to lateral forces or are neglected. Consequently, a similar approach will be followed as for the single vehicle but this time with

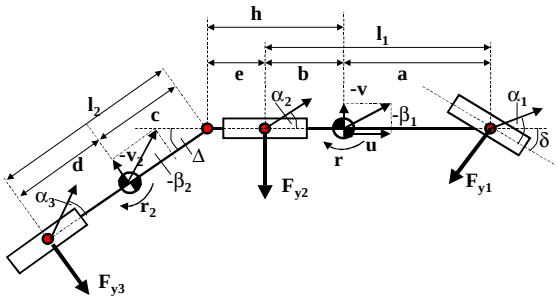

Figure 8.: Articulated vehicle model

the articulation angle Δ as an additional state. All wheels for one axle are taken as one system with overall characteristics and response. That means that tyre characteristics are again replaced by axle characteristics. Forward speed u is taken constant and pneumatic trails (i.e. aligning torques) are neglected.
Masses are denoted as m_1 for the first articulation (tractor, car) and m_2 for the second articulation (trailer, caravan,..). The polar moments of inertia are denoted as J_1 and J_2, respectively.

The equations of motion can be derived from the statements that equilibrium must hold in lateral and yaw direction. The lateral tyre forces must balance the lateral vehicle accelerations at both vehicle-parts. Moreover, the yaw moment acting on each of the articulations must be balanced by the moment due to the tyre forces plus the moment resulting from the internal reaction force at the articulation point. This leads to the equations (see figure 8 for notation):

$$(m_1+m_2)(\dot{v}+ur)-m_2[(h+c).\dot{r}-c\ddot{\Delta}]=F_{y1}+F_{y2}+F_{y3}$$
$$[J_1+m_2.h(h+c)]\dot{r}-m_2.h.[\dot{v}+ur+c\ddot{\Delta}]=a.F_{y1}-b.F_{y2}-h.F_{y3}$$
$$(J_2+m_2.c^2).(\ddot{\Delta}-\dot{r})+m_2.c.[\dot{v}+ur-h.\dot{r}]=(c+d).F_{y3}$$

in terms of lateral speed v and yaw rate r, both of the first vehicle (tractor), and the articulation angle Δ. The slip angles ate the three axles are derived similar to (8), leading to:

$$\alpha_1=\delta-\frac{v+a.r}{u}$$
$$\alpha_2=-\frac{v-b.r}{u} \qquad (9)$$
$$\alpha_3=-\Delta-\frac{v-(h+l_2).r+l_2.\dot{\Delta}}{u}$$

We'll discuss first the **steady state** situation, where the above equations reduce to:

$$(m_1+m_2).ur=F_{y1}+F_{y2}+F_{y3}$$
$$-m_2.h.ur=a.F_{y1}-b.F_{y2}-h.F_{y3} \qquad (10)$$
$$m_2.c.ur=(c+d).F_{y3}$$

and

$$\alpha_3=-\Delta-\frac{v-(h+l_2).r}{u} \qquad (11)$$

Observe that

$$\alpha_2-\alpha_3=\Delta-\frac{(e+l_2)}{R} \qquad (12)$$

Finding expressions for the lateral axle forces, one finds similar to (6) for the normalised axle characteristics that

$$f_{y1}=f_{y2}=f_{y3}=\frac{K}{m.g} \qquad (13)$$

which can again be inverted leading to multi-valued functions of α_i in terms of K/(mg). That means that a handling diagram can be established giving steady state solutions in terms of α_1 - α_2 and lateral acceleration a_y for given steering angle δ just as this was established earlier. At the right-hand side of the diagram, one draws a_y versus l_1/R with path radius of curvature R according to:

$$\frac{K}{mg}=\left(\frac{u^2}{g.l_1}\right)\frac{l_1}{R} \qquad (14)$$

In the same figure, a handling diagram can be established giving steady state solutions in terms of α_2 - α_3 and lateral acceleration a_y for given articulation angle Δ. At the right-hand side of the diagram, one now draws a_y versus $(l_2 + e)/R$ (as suggested by (12)):

$$\frac{K}{mg}=\left(\frac{u^2}{g.(l_2+e)}\right)\frac{l_2+e}{R} \qquad (15)$$

For a typical case of a tractor-trailer with normalised tyre characteristics as shown in figure 9, this analysis has been carried out, with the result depicted in figure

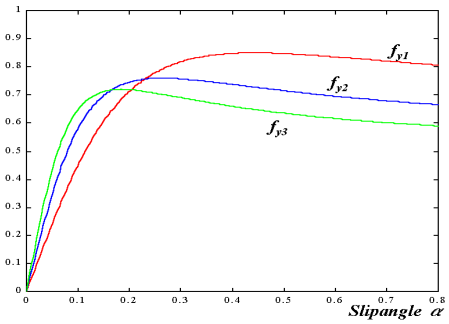

Figure 9.: Normalized axle characteristics

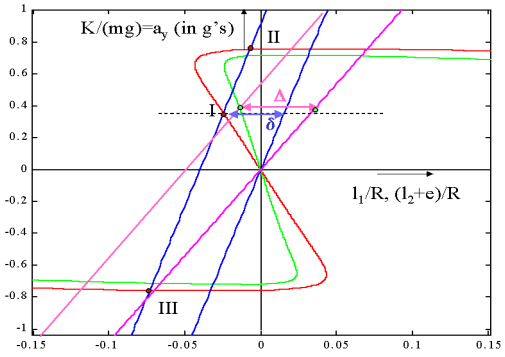

Figure 10.:Handling diagram articulated vehicle

10. The handling curve related to first and second axle is shown in red. The handling curve related to the second and the third axle is shown in green.
The tyre characteristics were chosen to obtain an illustrative handling diagram. The parameters as chosen for vehicle and vehicle input are listed in table 1, below.

a (m)	b (m)	c (m)	d (m)	e (m)
1.5	2.5	6.0	3.0	-0.5
m1(kg)	m2(kg)	δ (rad)	u (m/s)	
5000	20000	0.06	20	

Table 1.: Parameters, tractor-semitrailer

Two straight lines are shown, blue and purple relating to (14) and (15), respectively. Shifting the first over a steering angle δ and intersecting with the handling curve for the axles 1 and 2, leads to three steady state solutions, one of which is stable in yaw (I). As discussed above, this solution determines the lateral acceleration at hand, and from this the articulation angle being the horizontal distance between the straight line according to (15) and the α_2 -α_3 curve.

Having determined the steady state solutions in this graphical way, one may consider their stability. The handling diagram can be used to interpret yaw stability and divergent yaw-instability. Oscillating phenomena require a full treatment of the linearised equations of equilibrium. In figure 10, one may conclude just like for the single vehicle in the preceding section, that increasing the lateral acceleration starting from situation I implies that the steering angle δ must increase as well. At the same time, the articulation angle Δ will increase as well. That means that for both the tractor and the trailer, there is a compensating effect for the increased lateral acceleration and this effect was related to stability in the preceding section.

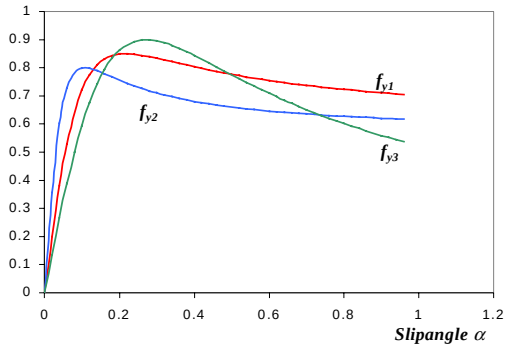

Figure 11.: Normalized axle characteristics, trailer oversteered

We shall continue with cases where at either the tractor or the trailer, these conclusions cannot be drawn.
Replace normalized tyre characteristics such that the highest cornering stiffness is obtained at the second axle and the lowest cornering stiffness is obtained at the rear axle. These characteristics are shown in figure 11. That means that for limited lateral acceleration, the tractor as a single vehicle, is understeered whereas the trailer with the second axle regarded as its leading and steering axle can be regarded as oversteered. Two handling diagrams (enlarged) have been determined for input steering angle 0.05 rad. and different speeds:

u_1 = 18 m/s
u_2 = 40 m/s.

The handling diagrams are shown in figures 12 and 13.

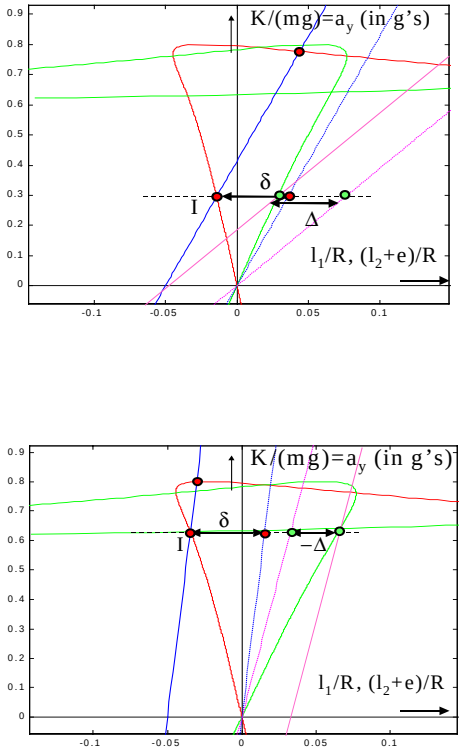

Figure 13.: Handling diagram, u=40 m/s

Again, take the steady state solution as starting point and consider steady state solutions for slightly larger lateral accelerations. That means that the steady state point will move up in the figures. In both figure 12 and 13 the steering angle δ will have to increase. However, considering the articulation angle Δ, this

angle appears to change sign for vehicle speed changing from 18 m/s to 40 m/s. Starting from both steady state solutions, the angle Δ will increase with increasing a_y in figure 12 whereas it will decrease with increasing a_y in figure 13. Consequently, in the last case, the trailer points inward and tries to follow a smaller path radius. Observe that steering angle and articulation angle have opposite signs. Apparantly, the trailer 'runs the show' in determining the vehicle performance, where the understeered nature of the tractor keeps the vehicle stable. As soon as the critical lateral acceleration is reached (where the tractor becomes oversteered), divergent instability will occur, controlled by the trailer. Compare this situation with figure 12 for low speed where steering angle and articulation angle both have the same sign, i.e. the tractor dominates the behaviour and the trailer follows the tractor response.

To get an understanding of all possible types of instability, we shall draw similar plots as figure 7, i.e. $F_{y2,\alpha}$ versus $F_{y1,\alpha}$ for various values of $F_{y3,\alpha}$. We shall do that for two typical vehicle configurations:

i. Tractor – semitrailer
ii. Truck with centre-axle trailer

The data used for both configurations is shown in table 2 and 3 below, with A_i denoting the values for axle cornering stiffness, setting the boundaries of the stability plot:

$$-A_i/4 < F_{yi,\alpha} < A_i$$

That means that we shall also consider negative slope of the axle characteristics under steady state conditions, ofcourse corresponding to the case of full sliding at that axle.

m1(kg)	m2(kg)	a(m)	l_1(m)	c(m)
5000	20000	1.5	4	6
l_2 (m)	e(m)	A_1(N)	A_2(N)	A_3(N)
9	-0.5	3.8E5	7.5E5	1.3E6

Table 2.: Parameters, tractor-semitrailer

m1(kg)	m2(kg)	a(m)	l_1(m)	c(m)
8000	20000	4	8	4
l_2 (m)	e(m)	A_1(N)	A_2(N)	A_3(N)
4	0.5	4E5	3E5	2E6

Table 3.: Parameters, truck & centre-axle trailer

We'll discuss first the impact of moving the cog of the trailer backward up to c = 8 m. Assuming linear tyre behaviour with the cornering stiffness equal to A_i, root-locus plots for varying speed u have been established for c = 6 m (reference case) and c = 8 m ($cog_{trailer}$ moved backward), see figure 14. For small value of c, two types of eigenvalues turn out to exist, real ones and complex ones, corresponding to the

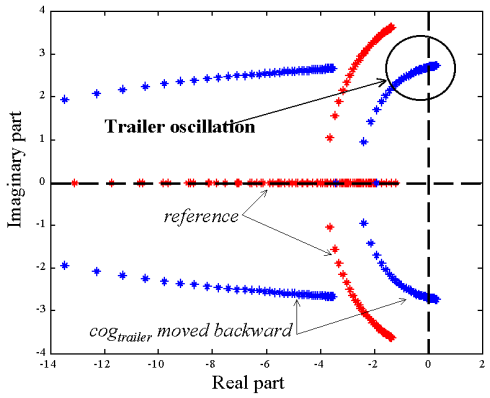

Figure 14.: Root-locus plot tractor-semitrailer

motion of the tractors and the semitrailer, respectively. Moving the cog of the trailer backward will make the vehicle combination unstable in the trailer-mode, indicating trailer oscillations beyond a certain speed. The corresponding cornering stiffness plot for u = 30 m/s is shown in figure 15, i.e. where the type of stability is indicated as a function of the actual slope of the lateral axle force, assuming full non-linear axle characteristics. This slope at the

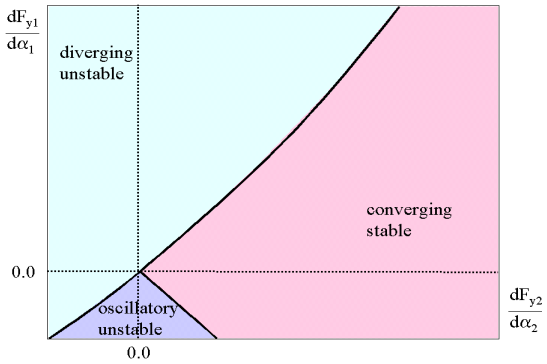

Figure 15.: Stability areas, reference case

semitrailer axle is taken according to table 2 (A_3). Note that the scales along both axes are not the same (cf. values of A_i in table 2)

This plot clearly corresponds to figure 7, with a stable area in the first quadrant, moving to divergent instability for decreasing slope of the lateral force at axle 2 (saddle point for a single vehicle), and moving to oscillatory instability for small negative slope at

axle 1. The same plot for the cog of the trailer moved backward is shown in figure 16.

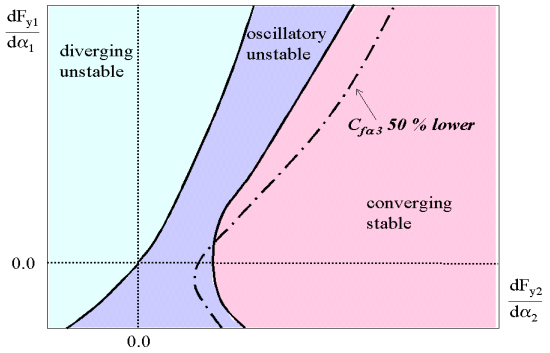

Figure 16.: Stability areas, $cog_{trailer}$ moved backward

This plot shows a strong increase of the oscillatory instability area, corresponding to behaviour of the trailer and confirming the occurrence of trailer oscillations around specific unstable steady state solutions. We have further decreased the slope of the trailer axle lateral force with 50 %. This resulted in a

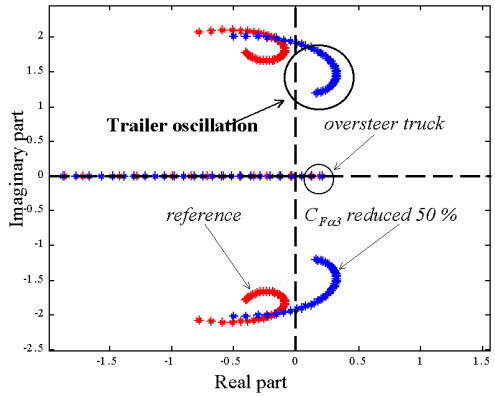

Figure 17.: Root-locus plot truck with centre-axle trailer

new boundary between the convergent stability area and the oscillatory instability area, indicated by a dash-dotted line. Consequently, the instability area will increase which is obvious from the reduced stiffness against yaw-oscillations of the trailer.

Next, we treat the truck with centre axle trailer, according to the data in table 3. The axle characteristics have been chosen such that unstable oversteer will occur beyond a certain speed. We'll discuss the impact of reducing the cornering stiffness of the trailer axle. with 50 %. Again, first assuming linear tyre behaviour with the cornering stiffness equal to A_i as listed in table 3, root-locus plots for varying speed u have been established for A_3 = 2E6 N (reference case) and A_3 = 1E6, see figure 17. One observes divergent instability beyond a critical speed in the reference situations. Reducing the trailer axle cornering stiffness results in oscillatory instability at much lower velocity compared to the initiation of divergent instability (oversteer). The corresponding stability areas for u = 25 m/s in terms of the cornering

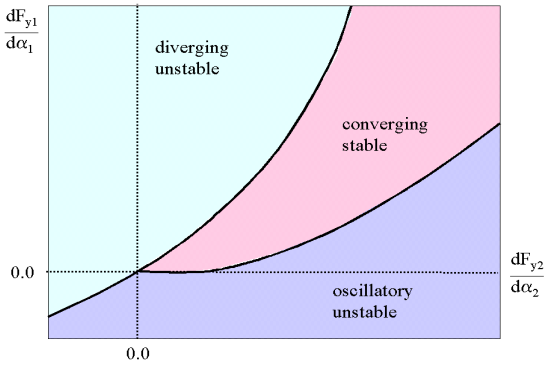

Figure 18.: Stability areas, centre-axle trailer, reference case

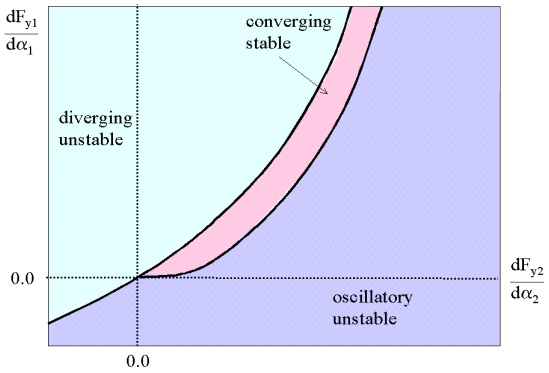

Figure 19.: Stability areas, centre-axle trailer, reduced cornering stiffnes trailer axle.

stiffnesses of the truck-axles are shown in figure 18 and 19, respectively.

One observes in figure 18 three different stability areas, with the stable combinations surrounded by divergent instability and oscillatory instability. Reducing the cornering stiffness at the trailer axle results in a significant reduction of the stability area, i.e. leaving only a stable solution for very specific combinations of slopes of the truck axle characteristics.

CONCLUSIONS.

In this paper, several tools have been used to analyse stability of nonarticulated and articulated commercial vehicles. All of these approaches confirm the strong impact of axle characteristics on vehicle performance, in combination with other vehicle parameters. Only simple models have been treated, based on the single track vehicle model. It is shown that the handling diagram concept, formerly extended from passenger cars to single trucks by Winkler, can be used to analyse articulated vehicles as far as nonoscillatory behaviour is concerned. With full nonlinear tyres, the type of (in-)stability can be nicely illustrated in a plot in terms of the slopes of the normalised lateral axle forces. This type of visualisation can be generalised to articulated vehicles as well, allowing a birds eye view of the combined impact of modified vehicle design and loading parameters and axle characteristics. This has been illustrated for some types of vehicle combinations.

REFERENCES

[1]. J.C. Dixon.: *Tires, Suspension and Handling.* SAE International, Arnold, a member of the Hodder Headline Group, London (1996).

[2]. L. Kusters.: *Increasing roll-over safety of commercial vehicles by application of electronic systems.* In.: J.P. Pauwelussen, H.B. Pacejka (eds.).: Smart vehicles. Swets & Zeitlinger Publishers, Amsterdam/Lisse, The Netherlands (1995)

[3]. H.B. Pacejka.: *Simplified analysis of steady state turning behaviour of motor-vehicles*, Veh. Sys. Dyn. 2, pp. 161 – 172 (1973)

[4]. H.B. Pacejka.: *Principles of plane motions of automobiles*, Proceedings of IUTAM Symposium on the Dynamics of Vehicles on Road and on Tracks, ed. H.B. Pacejka, Delft, pp. 33 – 59, Swets and Zeitlinger, Amsterdam (1976).

[5]. J.P. Pauwelussen: Analysis and prevention of excessive lateral behaviour of articulated vehicles. XII International Heavy Truck Conference, 13-15 September 1995, Budapest, Hungary

[6]. C.B. Winkler.: Simplified Analysis of the Steady-State Turning of Complex Vehicles. Vehicle System Dynamics, 29 (1998), pp. 141 – 180

[7]. J.v.d.Vegte.: *Feedback Control Systems*, Prentice-Hall International Editions, Englewood Cliffs (1990)